CONCLUSION

Tissue classification, based on a nearest neighbor algorithm, may be successfully utilized for volumetric analysis and growth rate determination. It may also provide a reliable and accurate method for determining change in contrast enhancing tissue. Thus the tissue classification method may play a role in determining response in therapeutic trials. It may provide information on the efficacy of therapeutic agents and may help to identify subgroups of patients particularly responsive to specific therapies. The prognostic value of growth rates, measured in terms of survival time, was significant ($p<0.03$) as was the CHO/CR measure ($p<0.02$). Finally, this study is currently engaged in understanding the relationship between growth rates and [^{1}H]-MRSI data, specifically CHO/CRE ratios.

ACKNOWLEDGMENTS

This work was made possible through the following grant support: NIMH/NIDA (P20 MH/DA52716), P41 NCRR (RR13642), NLM (LM/MH05633), NSF (BIR 93-22434), NCRR (RR05956) and NINDS/NIMH (NS38753); NCI CA 76524, ACS EDT-119.

REFERENCES

1. Djulbegovic B, Sullivan D, Decision Making in Oncology: Evidence Based Management. Churchill Livingstone, Philadelphia, pp 353-357.
2. Imperato JP, Paleologos NA, Vick NA. Effects of treatment on long-term survivors with malignant astrocytomas. Ann. Neurology 28:818-828, 1990.
3. Netsky MG, August B, Fowler W. The longevity of patients with glioblastoma multiforme. J Neurosurgery 7:261-269, 1950.
4. Talairach J, Tournoux P, *Co-planar Stereotaxic Atlas of Human Brain*. NY, NY: Thieme; 1988.
5. Evans AC, Collins DL, Neelin D, MacDonald D, Kamber M, Marrett S. Three-dimensional correlative imaging: applications in human brain mapping. *Functional Neuroimaging: Technical Foundation.* San Diego, Academic Press; 1994:145-162.
6. Mazziotta JC, Toga AW, Evans AC, Fox P, Lancaster J. A probabilistic atlas of the human brain: theory and rationale for its development. *Neuro Image*; 1995;2:89-101.
7. Sled J, Zijdenbos A, Evans A. A nonparametric method of automatic correction of intensity nonuniformity in the MRI Data. *IEEE Transactions on Medical Imaging*, 1998;17:87-97.
8. Thompson PM, Schwartz C, Toga AW. High resolution random mesh algorithm for creating a probabilistic atlas of the human brain, *NeuroImage*, 1996;3:19-34.
9. Clarke LP, Velthuizen RP, Clark M, et al. MRI measurement of brain tumor response: comparison of visual metric and automatic segmentation. *Magnetic Resonance Imaging*, 1998;16:271-279.
10. Clarke LP, Velthuzien RP, Camacho J, et al. MRI segmentation: methods and applications. Magnetic Resonance Imaging 1995;13:343-368
11. Bezdek J, Hall L, Clarke L. Review of MR image segmentation techniques using pattern recognition. *Medical Physics*, 1993;20;1033-47
12. Clarke LP, Velthuizen RP, Phuphanich S., Schellenberg J, Arrington J, Silbiger M. MRI: Stability of Three Supervised Segmentation Techniques. *Magnetic Resonance Imaging,* 1995;11:95-106.
13. Kaus M, Warfield S, Nabavi A, et al. Segmentation of meningiomas and low grade gliomas in MRI. *Proceedings of Second International Conference on Medical Image Computing and Computer-Assisted Interventions,* Cambridge, U.K 1999:1-10.
14. Sowell E, Thompson PM, Holmes C, Batth R, Jernigan T, Toga AW, Localized age-related changes in brain structures between childhood and adolescence using statistical parametric mapping *NeuroImage*, 1999;587-597.
15. Narr K, Thompson PM, Sharma T, Moussai J, Zoumalan C, Rayman J, Toga AW. 3D mapping of gyral shape and cortical surface asymmetries in schizophrenia: gender effects (In press).
16. Hammoud M, Sawaya R, Shi W, Thall P, Leeds N. Prognostic significance of preoperative MRI scans in glioblastoma multiforme. *Journal of Neuro-Oncology* 1996;27:65-73
17. Byar DP, Green SB, Strike TA. Prognostic factors for malignant glioma, in Walker MD (ed): *Oncology of the Nervous System*. Boston: Martinus Nijhoff, 1983, pp379-395.
18. Filipek P, Kennedy D, Caviness V. Volumetric analysis of central nervous system neoplasm based on MRI. *Pediatric Neurology*, 1991;7:347-351.
19. Chang L, McBride D, Miller BL, Cornford M, Booth RA, Buchthal SD, Ernst TM, Jenden D: Localized in vivo ^{1}H magnetic resonance spectroscopy and in vitro analysis of heterogeneous brain tumors. *J Neuroimaging* 5:157-163, 1995.
20. Miller BL, Chang L, Booth R, Ernst T, Conford M , Nikas D, McBride D, Jensed DJ. In vivo [^{1}H] MRS choline: Correlation with in vitro chemistry/histology. *Life Sci* 58:1929-1935, 1996.
21. Aiken NR, Gillies RJ. Phosphomonoester metabolism as a function of cell proliferative status and exogenous precursors. *Anti-cancer Research* 16:1393-1397, 1996.
22. Cuadrado A, Carnero A, Dolfi F, Jimenez B, Lacal JC. Phosphocholine, a novel second messenger essential for mitogenic activity. *Oncogene* 8:2959-2968, 1993.

adjustments in the prognosis of the patient.

As an extension of the second arm of this study we sought to correlate [^{1}H]-MRSI data, specifically CHO/CRE ratios, with tumor growth rates. MRS CHO data provide information on local cellularity and phosphocholine concentrations, thus reflecting the dynamics of differential cellular growth [19,20]. Phosphocholine is an important component of *de novo* membrane synthesis. High CHO concentrations in neoplastic tissue have been reported to be due to increased membrane turnover in dividing cells [21]. Recent data suggests that certain oncogenes can regulate the concentration of CHO-containing compounds and that some phosphocholine may be involved as second messengers in the modulation of growth factor-stimulated mitogenesis [22]. Linking [^{1}H]-MRS data, and the picture of cellular growth it provides, with growth rates determined through serially acquired volumetric analysis would further add to the value of the volumetric data. Thus far the data does not indicates a significant correlation between growth rates and CHO/CRE, even though each of these fators was separately corelated with survival. There are a number of possible reasons for this finding: 1) When compared with low grade tumors correlations between tumor growth rates and survival times may emerge; 2) Better quantitative methods, in part due to the strong partial volume effect of spectroscopy, might be needed to reveal a trend; 3) There may be no correlation between CHO/CRE and growth rates.

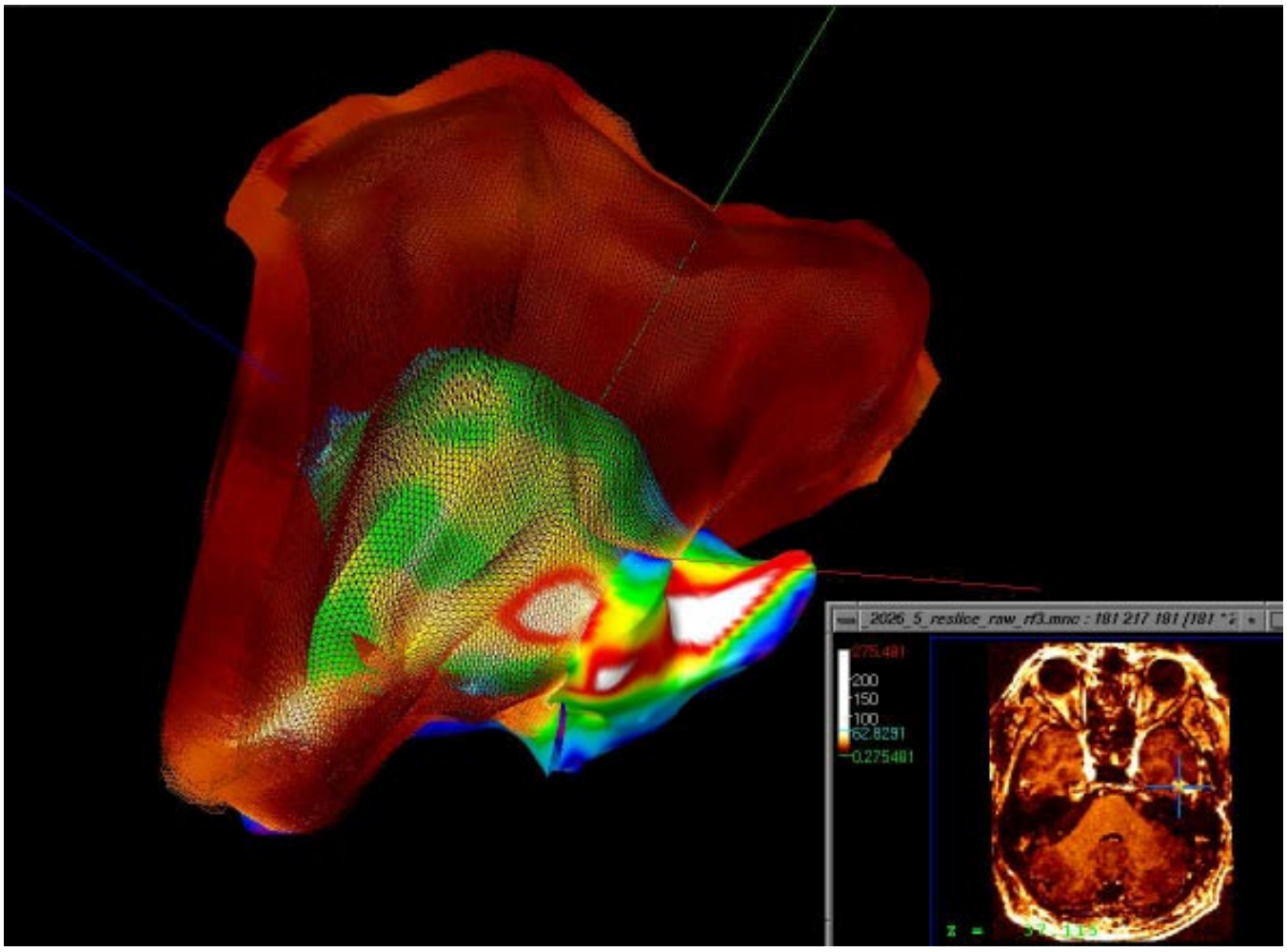

Fig. 6 Change may be tracked on a point-by-point basis with the surface modeling algorithm. The algorithm is able to follow focal growth while maintaining stereotaxic space. This provides a mechanism for accurately guiding biopsies to regions exhibiting differential growth. Genetic analysis may reveal inhomogeneities between the region of aggressive growth and the remainder of the tumor. Therapy may then be specifically tailored to the most aggressive regions.

between age at diagnosis and total survival time ($r=-0.54$, $p<0.03$). There was a significant negative correlation between growth rates, as determined from contrast enhancing tissue, and survival ($p<0.03$). A CHO/CRE of ≥ 1.8 was negatively correlated with survival ($p<0.02$). Growth rates and CHO/CRE may function as prognostic markers, ones which may be repeatedly acquired through the course of therapy. As such they may also be used to guide adjustments in therapy. Finally, no significant linear relationship was noted between growth rates and CHO/CRE values.

DISCUSSION

The ability to accurately and systematically track change in malignant gliomas is important, as is the identification of asociated prognostic factors. Enhancement volume provides an index to measure response to therapy, significant in the management of individual patients, and in assessing the efficacy of therapeutic agents during clinical trials. We analyzed the ability of two volumetric analysis approaches and validated the results against manually defined tumor enhancement volumes.

The tissue segmentation approach, based on a nearest neighbor algorithm, was shown to correlate well with manually defined contrast enhancing volume ($r^2=0.99$) and growth rates ($r^2=0.94$) (Fig. 4). Though the algorithm underestimated enhancement volumes it did so systematically and may therefore be applied reliably for enhancement volume estimation. The nearest-neighbor algorithm has been used in prior studies [9,10,11,12]. In Kaus et al. (1999), the algorithm accurately determined volumes of menigiomas and low grade astrocytomas [13]. The algorithm has certain advantages: (1) It provides stable segmentation [11,12,14,15]; (2) It is robust to changes in scanner protocol (TE, TR); (3) It is one of the most rapid algorithms in terms of execution times and operator input [11,12]; (4) The algorithm detects anatomically relevant structures while more automated algorithms may have greater difficulty [8,14].

The surface modeling algorithm has been used previously for detecting asymmetry in cortical patterns and for analyzing corpus callosum morphology in schizophrenic patients [14,15]. The surface modeling algorithm, in this study, was able to determine and track change in enhancement volume to a degree that was highly correlated with manually defined volumes ($r^2=0.94$). It was, however, unable to determine growth rates to the same high level of correlation. Despite its inability to determine growth rates with the same accuracy as the nearest neighbor algorithm, in specific cases the surface modeling algorithm may be better suited for tracking certain types of tumor changes. Because the surface modeling algorithm tracks change on a point-by-point basis, focal change may be observed. Since stereotaxic space is maintained, the surface modeling algorithm may provide a tool to guide biopsies from a specific region (Fig. 5). Genetic analysis of aggressive, or differentially growing, tumor regions may also reveal genetic heterogeneity in the tumor. Therapy, including combination therapy, could then be tailored to best suit the underlying genetics of the tumor.

It is worth noting that contrast enhancement represents the breakdown of the blood brain barrier and the extravasation of contrast enhancing material into the surrounding parenchyma, and not tumor proper itself. Contrast enhancement, therefore, may serve as an adjunct marker for tumor volume. Though both algorithms were able to track change in contrast enhancement, measures based on the tissue classification approach were more highly correlated to the manually defined volumes and growth rates than the surface modeling algorithm. Two reasons for this are: 1) Multiple lesions may be detected by tissue classification, while the surface modeling approach is limited to determining single contiguous volumes. 2) The volume determined by the surface modeling algorithm includes both contrast enhancing and necrotic areas while the tissue classification may distinguish enhancing regions from necrotic areas. The surface modeling algorithm has, for these two reasons, a tendency to underestimate or overestimate contrast enhancing volumes.

Monitoring edema is important for patient management. Further, moderate edema has been correlated with poor prognosis [16]. Edema was better quantified on T2-weighted images than T1-weighted images (where a 13.7% +/- 8.9% underestimation was observed). Manual determination of edema volumes was more successful than either algorithm. Less contrast between tissue and greater texture on T2-weighted images may have impaired the detection of edema by the tissue classification algorithm more. The RF-corrector, which assumes low-frequency signals are artifact, may also have failed to accurately detect edema due to interpretation of the edema signal as an inhomogeneity artifact.

Well-known prognostic markers for GBMs include: age, Karnofsky performance, and the extent of surgical resection [17]. Growth rates are also a marker sensitive enough to determine response to therapy [18]. As such they provide valuable insight into the efficacy of therapy and may provide enough information to make

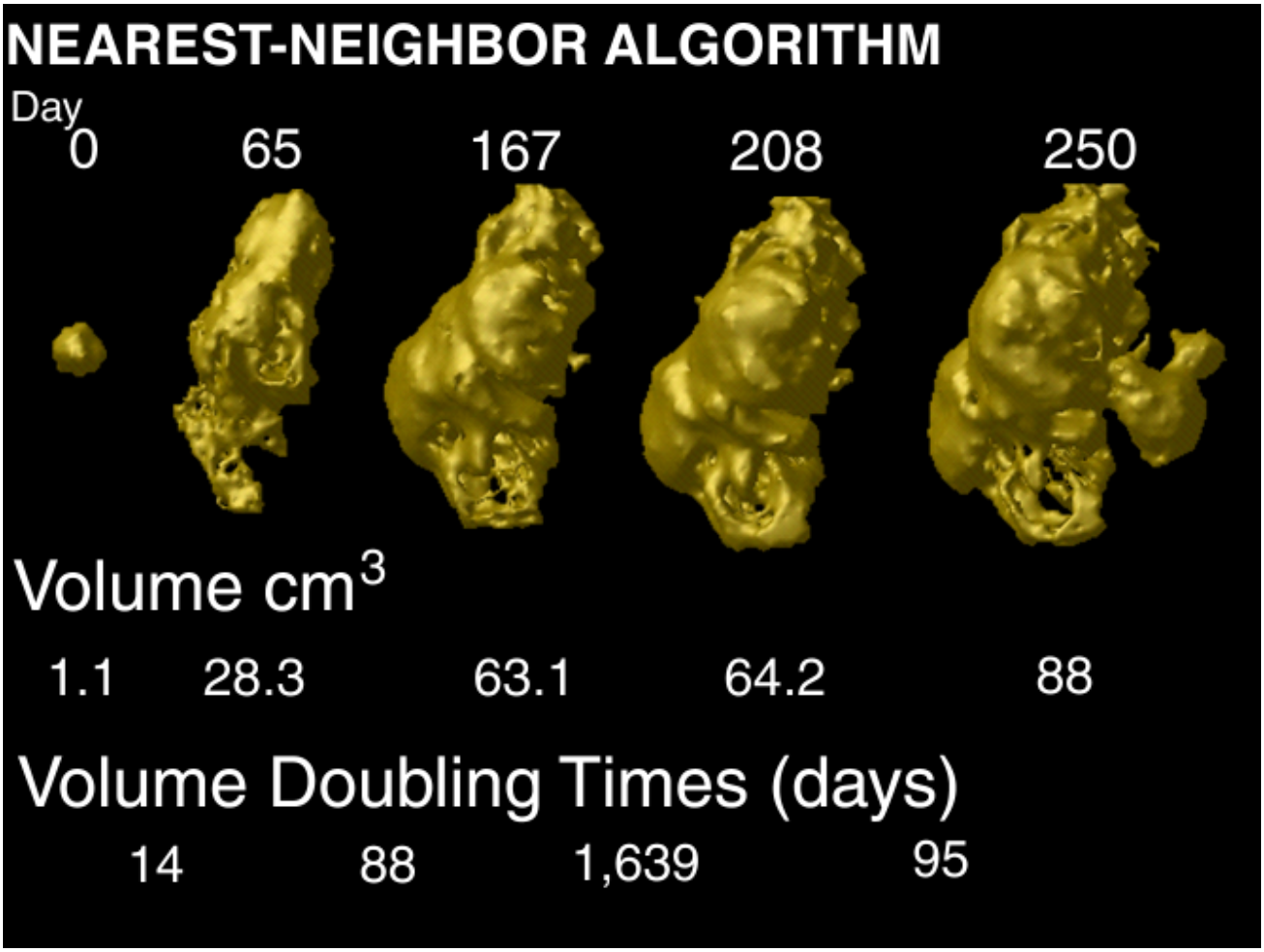

Fig. 5 The tissue classification method, based on the nearest neighbor algorithm, is able to systematically and reliably determine contrast enhancing tissue volumes. The approach could provide a way of determining efficacy of therapy in large scale, multi-center therapy trials..

RESULTS

Enhancement volumes, as determined by the tissue segmentation algorithm and the surface modeling algorithm, were both highly correlated with the manually defined volumes. The contrast-enhancing volumes as determined by the tissue segmentation algorithm had the following correlation: r^2=0.99 (manually defined 20.3cm^3 +/- SD 22.9; tissue segmentation algorithm mean 18.4 cm^3 +/- SD 22.1). The underestimation of enhancement volume was on average 9.4% when tissue segmentation was compared to manually-defined values. The correlation between the surface modeling algorithm and manually defined volumes was r^2=0.94 (manually defined 23.4cm^3 +/- SD 27.1; surface modeling algorithm mean 23.4cm^3 +/- SD 31.5; SD difference 4.4), values which approached the high correlation of the tissue segmentation algorithm.

Growth rates for tumor enhancement volumes were calculated in terms of estimated halving times and doubling times (Fig. 3). The growth rates as determined by the tissue segmentation algorithm were highly correlated with the growth rates as determined from the manually defined volumes (N=21, r^2=0.96; manually defined volumes 9.7 days, SD 99.8 days; algorithm means 8.5 days; SD 125.8 days). Nonetheless, growth rates as determined by the surface modeling algorithm correlated poorly with the manually defined growth rates.

Edema volumes from T1 and T2-weighted images were determined using the tissue segmentation algorithm and manual segmentation. T1-weighted manually segmented volumes systematically underestimated edema values as compared to T2-weighted images (by 13.7% +/- 8.9%). The tissue segmentation algorithm was unable to determine edema volumes systematically on either T1 or T2-weighted images.

A significant negative correlation was also found

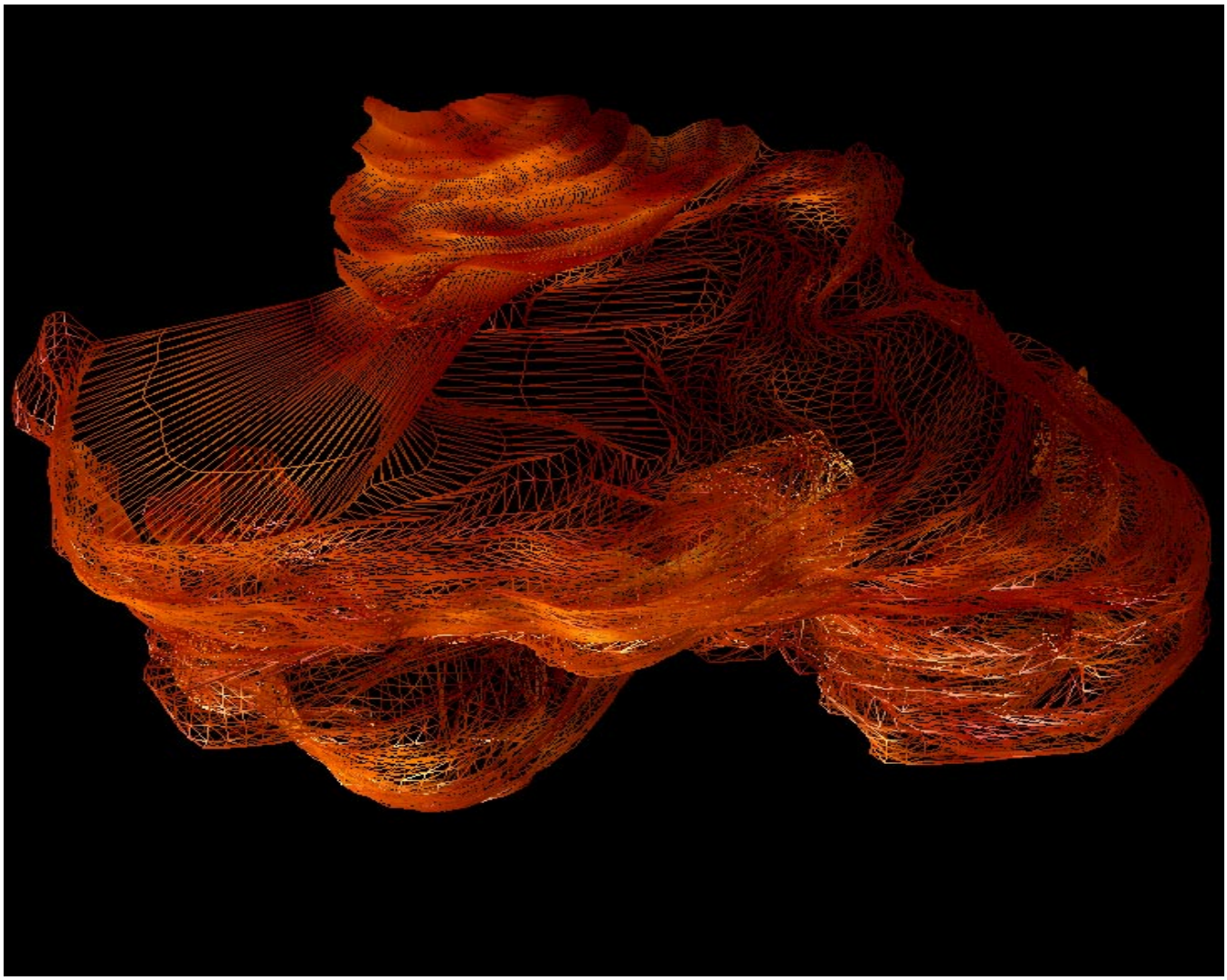

Fig.3 The result of the surface modeling algorithm is a parametric mesh model. The models may be rendered graphically, used to determine volumetric data, and, most importantly, track differential growth in tumor tissue.

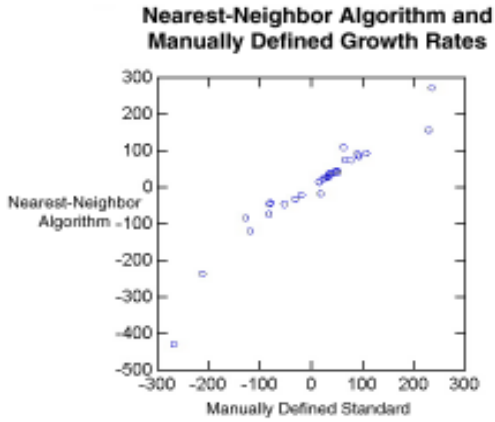

Fig. 4 Growth rates (mm^3/d) determined by the nearest neighbor algorithm were highly correlated with manually determined growth rates.

algorithm were compared to values determined from manually segmented images.

[^{1}H]-MRS data was processed on a Sun Sparc-20 computer (Sun Systems, Palo Alto, CA). The [^{1}H]-MRSI data were reconstructed from voxels within the imaged tissue. The five 3mm-thick MRI sections which corresponded to [^{1}H]-MRSI data were also reconstructed to create an MR image in register with the MRS image. Choline-creatine (CHO/CRE) ratios were obtained from active tumor and from tissue in the contralateral hemisphere.

Image Protocol

Images for this study were acquired using a 1.5 T MRI system (Signa 5.x Echospeed, General Electric Medical Systems, Milwaukee, WI). The following images were collected: T1-weighted volumes (TR/TE/NEX 550/8/2; slice thickness 3 mm, inter-slice gap 0, matrix 256 x 256, 25 cm field of view) and T2-weighted (TR/TE1/TE2/NEX 6000/14/126/2, slice thickness 3 mm, slice gap 0, 256 x 256 matrix). Post contrast T1-weighted images were acquired following the administration of Gadolinium DTPA, an MRI contrast agent (Magnevist, Berlex Laboratories, Wayne, NJ). The MRI scans obtained prior to the [^{1}H]-MRS study were used to constrain the acquisition of [^{1}H]-MRS slices. 'PRESS-CSI' and the echo-CSI (chemical shift imaging) acquisition software, provided by the manufacturer, were used to obtain the ^{1}H-MRSI data. The following parameters were utilized for the spectroscopic imaging: TR, 2000msec; TE, 272 msec; slice thickness 15 mm axial; field of view, 240 mm; in-plane phase encoded resolution, 24 x 24 or 32 x 32. Three specifically tailored frequency-selective saturating pulses were used prior to the acquisition of the spectroscopic data. The "short-tau-inversion recovery" (STIR) method was used for lipid suppression.

SGI 180 MHz R10000 workstations were used for aligning and segmenting the scans. Alignment was performed across MR submodalities and through the scan series by aligning image volumes into Talairach stereotaxic space using a 6-parameter rigid transformation [4]. Software developed at UCLA was used for manually assisted and automated registration.

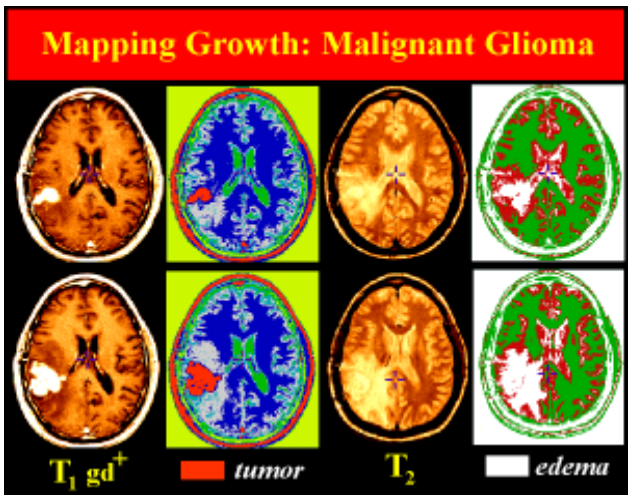

Fig. 1 This figure shows tissue segmentation maps for both tumor and edema generated by the tissue classification method.

Scans were manually aligned to a population-based average brain data set [5, 6]. All scans were RF-corrected to eliminate signal fluctuations due to distortions in the magnetic field of the scanner [7]. For the tissue segmentation algorithm the following protocol was followed: tags, 160 in all, representing points in white matter, gray matter, CSF, background, tumor and edema were chosen. Population-based tissue maps were used to perform tissue segmentation. Containing probabilistic information on tissue location in stereotaxic space, the population-based tissue maps were aligned to the scan data, adjusted for herniation effects with non-linear registration, and used to generate a Gaussian mixture distribution reflecting the intensities of specific tissue classes at each time point in the scan series. Tissue type was differentiated through the use of a nearest neighbor algorithm (Fig. 1). Tissue maps for tumor and edema were generated and manually adjusted so that class boundaries between tissue types were better delineated. For the surface modeling algorithm the following steps were performed: an operator defined the boundaries of the contrast enhancing tumor in serial sections. Traced points were converted by a surface modeling algorithm into a tiled parametric mesh model [8] (Fig 2.). This was accomplished by uniformly redigitizing the points at each level in adjacent sections and reconstructing the surface using triangular tiles (Fig. 3). Volumes were then determined from the mesh models. The tissue classification and the surface modeling

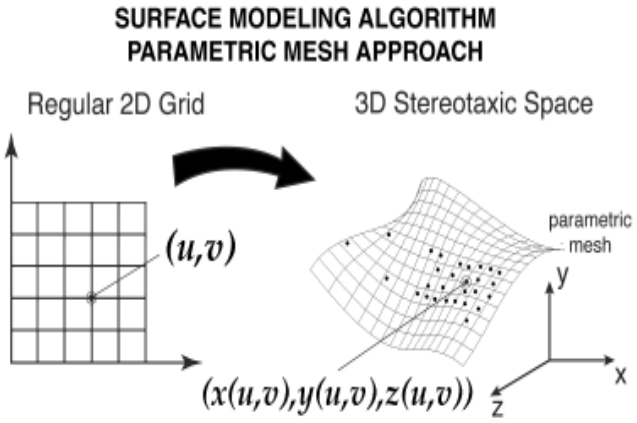

Fig. 2 The surface modeloing algorithm generates 3D parametric mesh models by uniformly redigitizing traced points. Points in adjacent 2D MR slices are joined using triangular tiles creating 3D volumes.

Cross Validation of Tissue Classification and Surface Modeling Algorithms for Determining Growth Rates of Malignant Gliomas: Prognostic Value of Growth Rates and MR Spectroscopy

[1]Haney S, [1]Thompson PM, [2 & 3]Cloughesy TF, [4]Alger JR, [4]Frew A,[1]Toga AW
[1]Laboratory of Neuro Imaging, Department of Neurology, Division of Brain Mapping; [2]Neuro Oncology Program,
[3]The Henry E. Singleton Brain Cancer Research Program, [4]Department of Radiological Sciences
UCLA School of Medicine, Los Angeles, CA 90095

ABSTRACT

A tissue classification method and a surface modeling algorithm were compared in their ability to analyze changes in brain tumors, based on volumetric MRI data. Measures were derived from serially acquired T2 and gadolinium-enhanced T1-weighted SPGR (spoiled Grass) MRIs. Volumes for contrast enhancing tissue, necrosis, and edema were determined and cross-validated against manually defined volumes. Volumes generated by both algorithms were highly correlated with volumes generated by manual segmentation (r^2=0.99 for the tissue segmentation method; r^2=0.96 for the surface modeling algorithm). Growth rates were calculated from contrast enhancing tissue volumes. Growth rates derived from the tissue classification approach were highly correlated with growth rates derived from manually segmented images (r^2=0.94). Growth rates were significantly correlated with survival ($p<0.03$) as was the choline to creatine ratio (CHO/CRE; $p<0.02$). [^{1}H]-MR spectroscopy measures, linked to the rates of cellular proliferation, were also examined to assess their relationship with growth rates.

Key Words: Brain, Tumor, Imaging, Algorithm, Growth Rate, MR Spectroscopy

INTRODUCTION

Malignancies of the central nervous system account for 1 percent of all cancers [1]. Though the percentage is small the impact on those patients with central nervous malignancies and their families is enormous. The prognosis for the *glioblastoma multiforme* (GBM), the most malignant of the nervous system neoplasms, is dismal; reported median survival is 50 weeks [2,3] . The ability to determine and track change in these tumors by imaging patients with contrast enhancement is important. Currently, there is no method for tumor quantification in widespread use. Identification of patients responding to therapies would be useful in planning not only therapies for individual patients but also in the assessment of therapeutic efficacy in large scale clinical trials. With improved assessment tools, better therapies could more rapidly be brought into clinical practice. Further, if patients could be identified with particular prognostic features therapies could be tailored to better suit the needs and desires of the individual patient. More effective treatments for specific patient subgroups shown to be more likely to respond favorably could be utilized, thereby avoiding less effective therapies associated with severe side effects and reduced quality of life.

As part of a comprehensive longitudinal study of patients with high grade gliomas we analyzed and cross-validated the performance of two algorithms in their ability to determine peritumoral edema, as well as the volume and growth rates of contrast enhancing tissue. We also assessed the correlation between growth rates and survival times. The algorithms tested were a tissue classification approach based on a nearest neighbor algorithm, and a surface modeling approach, in which parametric models of tumor boundaries are created. Further, MR spectroscopy was performed and the prognostic value of the spectroscopic data in relation to survival time and tumor growth rates was investigated.

METHODS

Fifteen patients with pathologically confirmed *glioblastoma multiforme* (GBM) were evaluated. Patients ranged in age from 18 to 64 (mean age 47.4 +/-12.8 yrs.) and were scanned longitudinally between 2 and 6 times over a period of up to 6 months. Prior to or during the scan interval patients underwent surgery and received either chemotherapy and radiation therapy or a combination of both.